Available online at www.sciencedirect.com

ScienceDirect

International Journal of Thermal Sciences 47 (2008) 811–819

International Journal of Thermal Sciences

www.elsevier.com/locate/ijts

Buoyant Couette–Bingham flow between vertical parallel plates

A. Barletta, E. Magyari [*,1]

Dipartimento di Ingegneria Energetica, Nucleare e del Controllo Ambientale (DIENCA), Università di Bologna, Via dei Colli 16, I-40136 Bologna, Italy

Received 30 April 2007; received in revised form 18 July 2007; accepted 19 July 2007

Available online 24 August 2007

Abstract

The present paper is closely related to a recent work of Bayazitoglu et al. [Y. Bayazitoglu, P.R. Paslay, P. Cernocky, Laminar Bingham fluid flow between vertical parallel plates, Int. J. Thermal Sci. 46 (2007) 349–357], in which the free convection of a Bingham material in a vertical parallel plane channel with a constant temperature differential across the walls has been investigated. Our interest is directed on the additional effect of an external shear, applied on the wall–fluid interface. This forcing shear is induced (in our mathematical model) by a uniform vertical motion of the hot wall of the channel in its own plane. The physically most interesting *five-domain configuration* of the velocity field of the resulting buoyant Couette–Bingham flow is examined in detail. For the *initiation temperature* of the flow, whose existence has been predicted in [Y. Bayazitoglu, P.R. Paslay, P. Cernocky, Laminar Bingham fluid flow between vertical parallel plates, Int. J. Thermal Sci. 46 (2007) 349–357], a generally valid formula is reported. Subsequently, it is shown that the core velocities with rigid body motion depend on the wall velocity sensitively. The hot and cold cores possess the same width which, however, decreases with increasing wall velocity rapidly. There always exists a critical downward pointing wall velocity for which the upward motion of the hot core is dropped.

Keywords: Bingham fluid; Vertical channel; Moving wall; Applied shear; Buoyant Couette flow

1. Introduction

This paper investigates the physical effect of external shear on the free convection of a Bingham fluid in a vertical parallel plane channel with a constant temperature differential across the walls. The additional shear is induced (in our mathematical model) by a uniform vertical motion of the hot wall of the channel in its own plane. It is found that the forcing effect of the applied shear affects both the configuration of the flow field and the magnitude of the core velocities of a Bingham fluid sensitively.

Our investigation was motivated by a recent paper of Bayazitoglu et al., [1], in which the *five-domain configuration* of the free convection velocity field of a Bingham material in a vertical channel with isothermal walls at different temperatures was examined in some detail. The investigation [1] was performed with regard to the flow of packer fluids (gels with Bingham behavior) in the annulus between the production tubing and the first production casing of oil and gas wells. To the description of the velocity field of the flow, an earlier solution reported by Yang and Yeh [2] was adapted.

In the free convection case the velocity field is symmetric with respect to the mid-plane of the channel. In the case of the present Couette–Bingham flow this symmetry gets broken. The reason for this feature resides in the non-symmetric velocity boundary conditions for the channel with a resting and a moving wall. Accordingly, the average flow velocity V_m (volumetric flow rate) through a section of the (full) channel is no longer vanishing. It is found that it equals the average velocity $(V_L + V_R)/2$ of the left and right cores with rigid body motion of the Bingham gel, which in turn equals the average velocity $(v_w + 0)/2 = v_w/2$ of the two walls of the channel, i.e. $V_m = (V_L + V_R)/2 = v_w/2$.

The paper is organized as follows. In Section 2, the model of Bayazitoglu et al., [1], is adapted to the no slip boundary conditions with a moving wall. In Section 3 the solution for the familiar case of the Newtonian fluid is described shortly. In Section 4 the solution for the five-domain configuration velocity

* Corresponding author.
E-mail address: magyari@hbt.arch.ethz.ch (E. Magyari).
1 On leave from ETH- Zürich, Switzerland.

1290-0729/$ – see front matter
doi:10.1016/j.ijthermalsci.2007.07.006

Nomenclature

C	constant of integration that equals the maximum of shear stress
D	constant of integration in equation of velocity
g	acceleration of gravity
H	distance between plates
KE/VOL	average kinetic energy per unit volume
k	thermal conductivity of fluid
Gr	Grashof number
$T'(x)$	temperature field
V_m	mean velocity in the full channel
V_L	velocity of the left hot core
V_R	velocity of the right cold core
v	local velocity in y-direction, a function of x
v_w	velocity of the left hot plate
x	coordinate across the gap, $x = 0$ is at hot plate, $x = H$ at cold plate
y	coordinate along the hot plate
ΔT	temperature differential across plates
β	thermal coefficient of volumetric expansion of the fluid
μ	dynamic viscosity
υ	kinematic viscosity, $\upsilon = \mu/\rho$
ρ	mass density of the fluid
ξ	dimensionless transversal coordinate, $\xi = x/H$
ξ_n	coordinates of interfaces between the five flow domains, $n = 1, 2, 3, 4$
τ_{xy}	shear stress in the flowing fluid
τ_{max}	maximum shear stress in the flowing fluid
τ_{min}	minimum shear stress in the flowing fluid
τ_*	gap between τ_{max} and τ_{min}
τ_0	yield point of the Bingham material model

field of the Couette–Bingham flow is given a closed analytical form. For the *initiation temperature* of the flow, of which existence has been predicted in [1], a generally valid formula is reported. Subsequently, the domain of existence of the solutions, the aiding and opposing effects of the applied shear on the flow, the effect of the wall velocity on the core velocities and core-widths, as well as comparison to Newtonian flow are discussed in Section 5. Section 6 summarizes the main results.

2. Governing equations

Consider the steady two-dimensional natural convection of a viscous fluid in a vertical parallel plane channel of width H. The walls are kept at constant temperatures $T_0 + \Delta T/2$ and $T_0 - \Delta T/2$, respectively, and the left (hot) wall moves with uniform velocity v_w in the y-direction (Fig. 1). We examine the parallel flow regime, in which the only non-vanishing component of the velocity field is its y-component $v = v(x)$. Following Bayazitoglu et al. [1], we assume that the Boussinesq approximation holds, and write the balance equations in the form

$$-\frac{dp'}{dx} + \rho g\beta T' + \frac{d\tau_{xy}}{dx} = 0 \tag{1a}$$

$$v\frac{\partial T'}{\partial y} = \alpha\left(\frac{\partial^2 T'}{\partial x^2} + \frac{\partial^2 T'}{\partial y^2}\right) \tag{1b}$$

where the fluid properties β and α are assumed to be constant and $p' = p - p_0$, $T' = T - T_0$ are the deviations of pressure and temperature from their values at hydrostatic condition. The present no slip and thermal boundary conditions are

$$v = v_w, \quad T' = \Delta T/2, \quad x = 0 \tag{2a}$$

$$v = 0, \quad T' = -\Delta T/2, \quad x = H \tag{2b}$$

As argued in [1], in the asymptotic state of the long-channel flow, the gradient of the pressure excess above the static pressure may be neglected and Eqs. (1a,b) of the velocity and temperature distribution reduce to

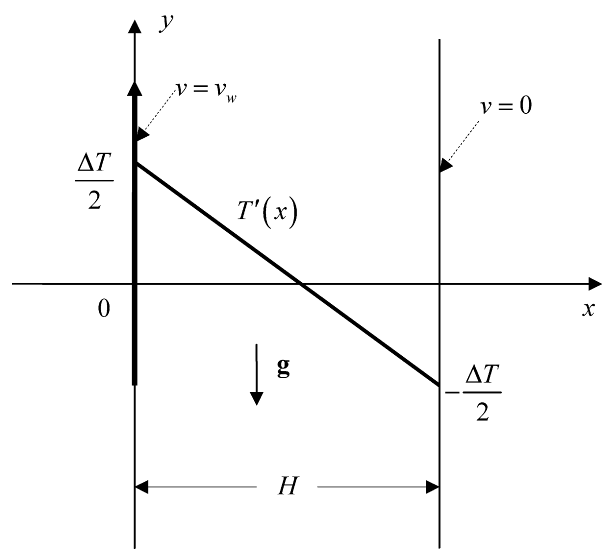

Fig. 1. Coordinate system and boundary conditions. The left hot wall of the channel is moving with uniform velocity v_w and the right cold one is at rest.

$$\rho g\beta T' + \frac{d\tau_{xy}}{dx} = 0 \tag{3a}$$

$$\frac{\partial^2 T'}{\partial x^2} = 0 \tag{3b}$$

It is admitted that Eqs. (3) hold, in a first approximation, also under the present boundary conditions.

The integration of Eq. (3b) along with the boundary conditions (2) gives the linear temperature distribution

$$T'(x) = \left(\frac{1}{2} - \xi\right)\Delta T \tag{4}$$

and the integration of Eq. (3a) yields for the shear stress the expression

$$\tau_{xy} = \frac{\rho}{2}\left(\frac{\upsilon}{H}\right)^2 Gr\left(\xi^2 - \xi\right) + C \tag{5}$$

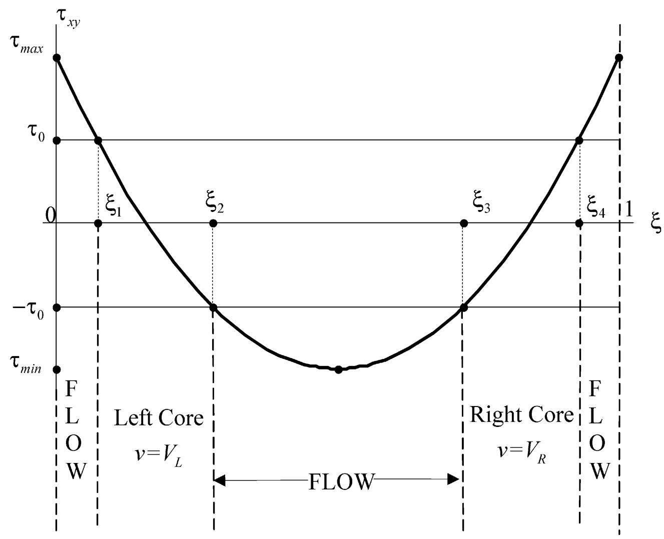

Fig. 2. Domains of viscous flow and of rigid body motion ("cores") of the Bingham gel.

where C is a constant of integration and υ denotes the kinematic viscosity, $\upsilon = \mu/\rho$. The dimensionless length ξ and the Grashof number Gr have been defined as follows

$$\xi = \frac{x}{H} \tag{6a}$$

$$Gr = \frac{g\beta \Delta T H^3}{\upsilon^2} \tag{6b}$$

Eq. (5) shows that $C = \tau_{xy}|_{x=0} = \tau_{xy}|_{x=H}$. At the same time, C represents the largest value of τ,

$$C = \tau_{\max} \tag{7}$$

The minimum of τ is reached for $\xi = 1/2$ and is

$$\tau_{\min} = \tau|_{\xi=1/2} = \tau_{\max} - \tau_* \tag{8}$$

where

$$\tau_* \equiv \frac{1}{8}\rho\left(\frac{\upsilon}{H}\right)^2 Gr = \frac{1}{8}\rho g H\beta\Delta T \tag{9}$$

represents the gap between the maximum and minimum value of τ_{xy} (see Fig. 2).

3. The Newtonian flow

The familiar case of the Newtonian viscous flow should serve here as a reference. The shear stress distribution (5) has to be substituted in this case into the linear viscous flow equation

$$\mu\frac{\mathrm{d}v}{\mathrm{d}x} = \tau_{xy} = 4\tau_*\left(\xi^2 - \xi\right) + C \tag{10}$$

Integrating Eq. (10) once, we obtain

$$v = \frac{\upsilon Gr}{12H}\left(2\xi^3 - 3\xi^2\right) + \frac{H}{\mu}C\xi + K \tag{11}$$

The constants of integrations C and K can be determined with the aid of the velocity boundary conditions (2). Thus we obtain for the velocity field and the shear stress distribution of the Couette flow in the vertical channel the explicit expressions

$$v = v_w(1-\xi) + \frac{\upsilon Gr}{12H}\left(2\xi^3 - 3\xi^2 + \xi\right) \tag{12}$$

$$\tau_{xy} = \frac{2}{3}\tau_*\left(6\xi^2 - 6\xi + 1 - \frac{12Hv_w}{\upsilon Gr}\right) \tag{13}$$

Accordingly,

$$\tau_{\max} = \frac{2}{3}\tau_*\left(1 - \frac{12Hv_w}{\upsilon Gr}\right) \tag{14}$$

and

$$\tau_{\min} = -\frac{1}{3}\tau_*\left(1 + \frac{24Hv_w}{\upsilon Gr}\right) \tag{15}$$

In the case of the resting wall ($v_w = 0$), we recover in (12)–(15) the results of Bayazitoglu et al. [1]. However, in contrast to the case $v_w = 0$ where the velocity field $v(x)$ shows a geometric symmetry with respect to the mid-plane $\xi = 1/2$ of the channel ($v(x)$ is an odd function of $x - H/2$), the mean velocity of the Couette flow through the full section of the channel is not zero but, as expected, is given by

$$V_m = \frac{1}{H}\int_0^H v(x)\,\mathrm{d}x = \frac{v_w}{2} \tag{16}$$

The average kinetic energy per unit volume, KE/VOL

$$\frac{KE}{VOL} = \frac{1}{H}\int_0^H \frac{1}{2}\rho v^2\,\mathrm{d}x \tag{17}$$

is calculated to be

$$\frac{KE}{VOL} = \frac{\rho}{60\,480}\left(\frac{\upsilon Gr}{H}\right)^2\left(1 + 7\varepsilon + 70\varepsilon^2\right) \tag{18a}$$

$$\varepsilon = \frac{12Hv_w}{\upsilon Gr} \tag{18b}$$

In this way, Eqs. (16) and (13) yield

$$\frac{KE/VOL}{\tau_{\max}} = \frac{Gr}{5040}\,\frac{1 + 7\varepsilon + 70\varepsilon^2}{1 - \varepsilon} \tag{19}$$

In the case of the resting wall ($v_w = 0$, i.e. $\varepsilon = 0$), we recover in (17) and (19) the results of Bayazitoglu et al. [1], again.

4. The Couette–Bingham flow

We consider the flow of a Bingham gel of yield stress τ_0. Following Bayazitoglu et al. [1], we focus our attention on the most interesting physical situation, which is specified by the inequalities

$$0 < \tau_0 < \tau_{\max}$$
$$\tau_{\min} < -\tau_0 < 0 \tag{20}$$

where $\tau_{\max}$ and $\tau_{\min}$ are related to the unknown integration constant C by Eqs. (7) and (8) (see Fig. 2). In this way inequalities (20) require

$$0 < \tau_0 < C < \tau_* \tag{21}$$

The coordinates $0 < \xi_1 < \xi_2 < \xi_3 < \xi_4 < 1$ of the interfaces between the viscous flow regions and the cores with rigid-body motion of the Bingham material are obtained in this case as roots of equations $\tau = \tau_0$ and $\tau = -\tau_0$, respectively, where τ is given by Eq. (5). Thus, equation $\tau = \tau_0$ yields

$$\xi_1 = \frac{1 - S_-}{2}, \qquad \xi_4 = 1 - \xi_1 \tag{22}$$

and equation $\tau = -\tau_0$ yields

$$\xi_2 = \frac{1 - S_+}{2}, \qquad \xi_3 = 1 - \xi_2 \tag{23}$$

where $S_\pm$ stand for the square root expressions

$$S_\pm = \sqrt{1 - \frac{\tau_0}{\tau_*}\left(\frac{C}{\tau_0} \pm 1\right)} = \sqrt{1 - 8\left(\frac{C}{\tau_0} \pm 1\right)\frac{\tau_0}{\rho g H}\frac{1}{\beta \Delta T}} \tag{24}$$

The constitutive equations in the five parallel-plane domains of Fig. 2 are

$$\mu \frac{\mathrm{d}v}{\mathrm{d}x} = \tau - \tau_0 \qquad \text{when } 0 \leqslant \xi \leqslant \xi_1 \tag{25}$$

$$v = V_L \text{ (left core)} \qquad \text{when } \xi_1 \leqslant \xi \leqslant \xi_2 \tag{26}$$

$$\mu \frac{\mathrm{d}v}{\mathrm{d}x} = \tau + \tau_0 \qquad \text{when } \xi_2 \leqslant \xi \leqslant \xi_3 \tag{27}$$

$$v = V_R \text{ (right core)} \qquad \text{when } \xi_3 \leqslant \xi \leqslant \xi_4 \tag{28}$$

$$\mu \frac{\mathrm{d}v}{\mathrm{d}x} = \tau - \tau_0 \qquad \text{when } \xi_4 \leqslant \xi \leqslant 1 \tag{29}$$

Concerning the velocity field of the Couette–Bingham flow, there occurs an essential difference comparing to the resting wall ($v_w = 0$) case investigated in [1]. This consists of the fact that, although the stress distribution (5) due to the buoyancy forces is symmetric with respect to the mid-plane $\xi = 1/2$ of the channel in both cases, in the case of Couette–Bingham flow the geometric symmetry of the velocity field of the case $v_w = 0$ gets broken. The simple reason for this feature resides in the non-symmetric velocity boundary conditions (2a) and (2b) for $v_w \neq 0$. Accordingly, in the case $v_w \neq 0$ the mathematical approach may not be restricted to the half-channel $0 \leqslant \xi \leqslant 1/2$ as being done in [1].

The differential equations (25), (27) and (29), with τ given by Eq. (5), can immediately be integrated. The constants of integration occurring in Eqs. (25) and (29) can be determined from the boundary conditions (2a) and (2b) easily. In this way, we obtain for the velocity field of the Couette–Bingham flow the expression

$$v = \begin{cases} \frac{\upsilon\, Gr}{12H}(2\xi^3 - 3\xi^2) + \frac{H}{\mu}(C - \tau_0)\xi + v_w \\ \quad \text{for } 0 \leqslant \xi \leqslant \xi_1 \\ V_L \quad \text{for } \xi_1 \leqslant \xi \leqslant \xi_2 \\ \frac{\upsilon\, Gr}{12H}(2\xi^3 - 3\xi^2) + \frac{H}{\mu}(C + \tau_0)\xi + \frac{H}{\mu}D \\ \quad \text{for } \xi_2 \leqslant \xi \leqslant \xi_3 \\ V_R \quad \text{for } \xi_3 \leqslant \xi \leqslant \xi_4 \\ \frac{\upsilon\, Gr}{12H}(2\xi^3 - 3\xi^2 + 1) + \frac{H}{\mu}(C - \tau_0)(\xi - 1) \\ \quad \text{for } \xi_4 \leqslant \xi \leqslant 1 \end{cases} \tag{30}$$

where D is a constant of integration.

The continuity requirement of the velocity in the planes $\xi = \xi_n$, $n = 1, 2, 3, 4$, of the flow field leads to the equations (matching conditions)

$$\frac{\upsilon\, Gr}{12H}\left(2\xi_1^3 - 3\xi_1^2\right) + \frac{H}{\mu}(C - \tau_0)\xi_1 + v_w = V_L \tag{31}$$

$$\frac{\upsilon\, Gr}{12H}\left(2\xi_2^3 - 3\xi_2^2\right) + \frac{H}{\mu}(C + \tau_0)\xi_2 + \frac{H}{\mu}D = V_L \tag{32a}$$

$$\frac{\upsilon\, Gr}{12H}\left(2\xi_3^3 - 3\xi_3^2\right) + \frac{H}{\mu}(C + \tau_0)\xi_3 + \frac{H}{\mu}D = V_R \tag{33a}$$

$$\frac{\upsilon\, Gr}{12H}\left(2\xi_4^3 - 3\xi_4^2 + 1\right) + \frac{H}{\mu}(C - \tau_0)(\xi_4 - 1) = V_R \tag{34}$$

These four equations, where the ξ_n's are given by Eqs. (22)–(24), determine basically the four unknown quantities C, D, V_L and V_R of the problem in terms of the input data v_w, τ_0, H and ΔT. Having in mind the second equation (22), $\xi_4 = 1 - \xi_1$, the sum of Eqs. (31) and (34) gives the relationship

$$V_L + V_R = v_w \tag{35}$$

Similarly, having in mind the second equation (23), $\xi_3 = 1 - \xi_2$, the sum of Eqs. (32a) and (33a) leads to the relationship

$$-\frac{\upsilon\, Gr}{12H} + \frac{H}{\mu}(C + \tau_0) + \frac{2H}{\mu}D = V_L + V_R \tag{36}$$

which, along with Eq. (35), furnishes for D the expression

$$D = \frac{\mu}{2H}\left[v_w + \frac{\upsilon\, Gr}{12H} - \frac{H}{\mu}(C + \tau_0)\right] \tag{37}$$

Substituting Eq. (37) in Eq. (30), the velocity field becomes

$$v = \begin{cases} \frac{\upsilon\, Gr}{12H}(2\xi^3 - 3\xi^2) + \frac{H}{\mu}(C - \tau_0)\xi + v_w \\ \quad \text{for } 0 \leqslant \xi \leqslant \xi_1 \\ V_L \quad \text{for } \xi_1 \leqslant \xi \leqslant \xi_2 \\ \frac{\upsilon\, Gr}{12H}(2\xi^3 - 3\xi^2 + \frac{1}{2}) + \frac{H}{\mu}(C + \tau_0)(\xi - \frac{1}{2}) + \frac{v_w}{2} \\ \quad \text{for } \xi_2 \leqslant \xi \leqslant \xi_3 \\ V_R \quad \text{for } \xi_3 \leqslant \xi \leqslant \xi_4 \\ \frac{\upsilon\, Gr}{12H}(2\xi^3 - 3\xi^2 + 1) + \frac{H}{\mu}(C - \tau_0)(\xi - 1) \\ \quad \text{for } \xi_4 \leqslant \xi \leqslant 1 \end{cases} \tag{38}$$

Furthermore, on account of Eq. (37), the matching conditions (32) and (33) become

$$\frac{\upsilon\, Gr}{12H}\left(2\xi_2^3 - 3\xi_2^2 + \frac{1}{2}\right) + \frac{H}{\mu}(C + \tau_0)\left(\xi_2 - \frac{1}{2}\right) + \frac{v_w}{2} = V_L \tag{32b}$$

$$\frac{\upsilon\, Gr}{12H}\left(2\xi_3^3 - 3\xi_3^2 + \frac{1}{2}\right) + \frac{H}{\mu}(C + \tau_0)\left(\xi_3 - \frac{1}{2}\right) + \frac{v_w}{2} = V_R \tag{33b}$$

There are two straightforward ways to obtain an equation for determination of C, namely, by combining Eqs. (31) and (32b) or Eqs. (33b) and (34). Owing to the relationships $\xi_3 = 1 - \xi_2$ and $\xi_4 = 1 - \xi_1$, these procedures are obviously equivalent and result in equation

$$\frac{2}{3}\frac{\tau_*}{\tau_0}\left(2\xi_1^3 - 3\xi_1^2 - 2\xi_2^3 + 3\xi_2^2 - \frac{1}{2}\right) + \left(\frac{1}{2} + \xi_1 - \xi_2\right)\frac{C}{\tau_0} + \frac{1}{2} - \xi_1 - \xi_2 + \frac{\mu v_w}{2\tau_0 H} = 0 \tag{39}$$

In terms of the square root expressions (24), Eq. (39) can be transcribed in the form

$$v_w = \frac{\upsilon\, Gr}{24H}\left(2S_+^3 - 2S_-^3 + 3S_-^2 - 1\right) \tag{40}$$

Eqs. (31) and (34) of the core velocities can similarly be transcribed in the form

$$V_L = \frac{v_w}{2} + \frac{\upsilon\, Gr}{24H} S_+^3$$
$$V_R = \frac{v_w}{2} - \frac{\upsilon\, Gr}{24H} S_+^3 \tag{41}$$

Once the transcendental equation (40) has been solved for C, the value of the core velocities can be calculated from Eqs. (41), and thus the velocity field is determined according to Eq. (38) completely. The corresponding shear distribution results from Eq. (5). The average velocity of the Bingham gel in the (full) channel calculated with the aid of Eqs. (38) and (35) is obtained as

$$V_m = \frac{v_w}{2} = \frac{V_L + V_R}{2} \tag{42}$$

In other words, the average velocity of the Bingham gel is equal to the average velocity of the two cores with solid body motion on the one hand, and with the average velocity (16), $V_m = v_w/2$, of the Newtonian fluid, on the other hand.

5. Discussion

5.1. Existence range of the five-domain flow configurations

The key task in discussing the features of the five-domain velocity field (38) of the Couette–Bingham flow, is to obtain the solution of the transcendental equation (40) for C when the values of all the other quantities involved are given. The main results concerning the domain of existence of the solutions will be given in a generally valid analytical form. However, in order to be more specific, we chose for illustration the parameter values $H = 0.025$ m, $\rho = 1100$ kg/m^3, $\mu = 0.002$ kg/(m s), $\tau_0 = 2.5$ kg/(m s^2) which are close to those of the example discussed by Bayazitoglu et al. [1]. Concerning the range of values of $\beta\Delta T$, we also assume with Ref. [1] that

$$0 \leqslant \beta\Delta T \leqslant 0.22 \tag{43}$$

For a given value of the wall velocity v_w, the solution of Eq. (40) for the ratio C/τ_0 corresponds according to the inequalities (21) to the physical situation assumed in Fig. 2, only when it satisfies the conditions

$$1 < \frac{C}{\tau_0} < \frac{\tau_*}{\tau_0} \tag{44}$$

It can be shown that the right-hand side of Eq. (40) is a real quantity only in the range

$$\frac{C}{\tau_0} \leqslant \frac{\tau_*}{\tau_0} - 1 \tag{45}$$

and becomes imaginary for $C/\tau_0 > (\tau_*/\tau_0) - 1$. Thus, the physical situation of the five-domain flow configuration of Fig. 2, is actually specified by the more restrictive conditions

$$1 < \frac{C}{\tau_0} \leqslant \frac{\tau_*}{\tau_0} - 1 \tag{46}$$

These inequalities require in turn that $\tau_*/\tau_0 \geqslant 2$ which, according to Eq. (9) of τ_*, implies that there always exists a smallest value $\beta\Delta T$,

$$(\beta\Delta T)_{\min} = \frac{16\tau_0}{\rho g H} \tag{47}$$

below which no five-domain flow configurations can exist. For the minimum value (47) of $\beta\Delta T$ (i.e., for $\tau_*/\tau_0 = 2$) the unique solution of Eq. (40) is ($/\tau_0 = 1$, $v_w = 0$). We mention that the existence of a lowest bound for the initiation temperature of the five-domain Bingham flow has already been predicted by Bayazitoglu et al. [1]. With the present choice of the parameters (and $g = 9.81$ m/s^2) one obtains from Eq. (47) the value $(\beta\Delta T)_{\min} = 0.148272$.

The above flow features are illustrated in Fig. 3, where the wall velocity v_w has been plotted according to Eq. (40), as a function of the ratio C/τ_0 for four different values of $\beta\Delta T$ in the range $(\beta\Delta T)_{\min} \leqslant \beta\Delta T \leqslant 0.22$. The dots at the lower end of the curves mark the right limit of the existence domain of real solutions, which are specified by the equality case of Eq. (46) and have the coordinates $(C/\tau_0, v_w) = (1.42798, -0.60793)$, $(1.69775, -1.47747)$ and $(1.96753, -2.61806)$ for $\beta\Delta T = 0.18, 0.20$ and 0.22, respectively. In the dots on the horizontal axis, we recover the solutions discussed by Bayazitoglu et al. [1], which correspond to the resting wall ($v_w = 0$) and which are located in the present case at $C/\tau_0 = 1$, 1.33610, 1.53265 and 1.72488, for $\beta\Delta T = 0.148272$, 0.18, 0.20 and 0.22, respectively. Furthermore, the dots on the dashed vertical line at $C/\tau_0 = 1$ mark according to Eq. (46) the left limit of the existence domain of solutions corresponding to the physical situation shown in Fig. 2. Their coordinates are $(C/\tau_0, v_w) = (1, 3.74338), (1, 7.39278)$ and $(1, 11.5095)$ for $\beta\Delta T = 0.18, 0.20$ and 0.22, respectively. Therefore the existence domain of the solutions extends for $\beta\Delta T > (\beta\Delta T)_{\min}$ both to positive and negative values of the wall velocity, i.e. to

$$\begin{aligned}
-0.60793 &\leqslant v_w\ [\text{m/s}] < 3.74338 \quad \text{for } \beta\Delta T = 0.18\\
-1.47747 &\leqslant v_w\ [\text{m/s}] < 7.39278 \quad \text{for } \beta\Delta T = 0.20\\
-2.61806 &\leqslant v_w\ [\text{m/s}] < 11.5095 \quad \text{for } \beta\Delta T = 0.22
\end{aligned} \tag{48}$$

It is worth mentioning here that the dots on the dashed vertical line at $C/\tau_0 = 1$ do not belong in fact to the existence domain of the solutions with five different flow regions (the interval (46) is open at its left side). This is also clearly seen in Fig. 2, where the two outer flow domains disappear as τ_0 approaches the value of C, i.e. the five-domain structure of the flow field reduces to a three-domain one.

5.2. Aiding and opposing effects of the applied shear

Concerning the effect of the shear induced by the moving wall, the following aspects should be emphasized. In the case $v_w > 0$ the shear due to the upward moving hot wall does assist the buoyancy forces in its neighborhood. Accordingly, the velocity $V_L > 0$ of the (left) hot core must become larger compared to the case $v_w = 0$. At the same time, the shear forces induced by the upward moving hot wall are opposite to the

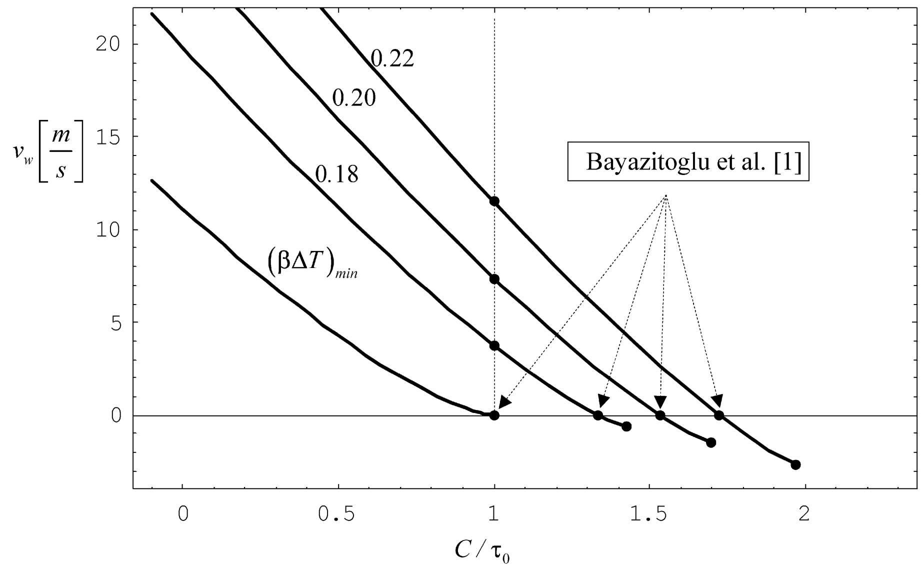

Fig. 3. Plot of the wall velocity v_w as a function of the ratio C/τ_0 for the four indicated values of $\beta\Delta T$, where $(\beta\Delta T)_{\min} = 0.148272$.

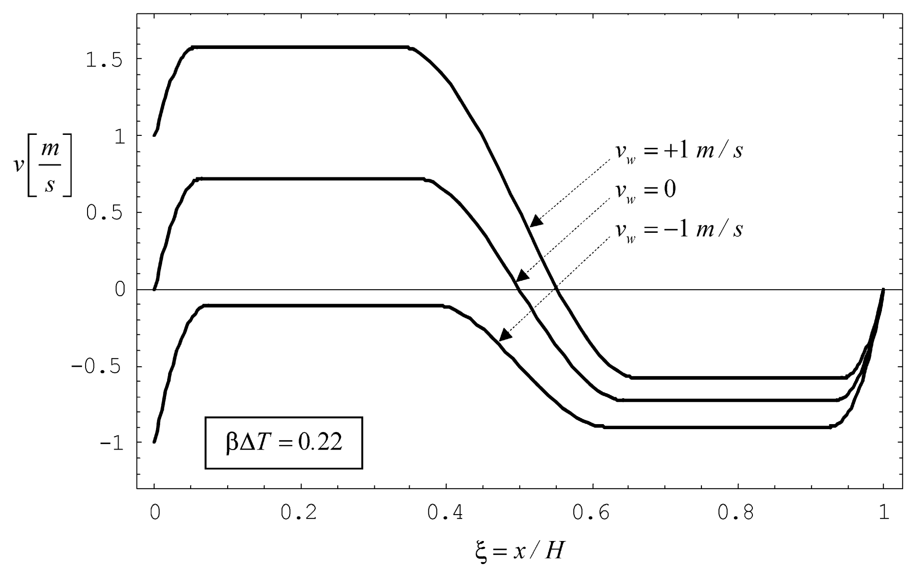

Fig. 4. Plot of the velocity profiles (38) for $\beta\Delta T = 0.22$ and the wall velocities $v_w = 1$ m/s, $v_w = 0$ and $v_w = -1$ m/s, respectively. In the two former cases the velocity field is bidirectional and in the latter one unidirectional.

buoyancy forces in the neighborhood of the cold right wall. Accordingly, the magnitude $|V_R|$ of the velocity $V_R < 0$ of the (right) cold core must become smaller compared to the case $v_w = 0$. Obviously, in the case $v_w < 0$ of the downward moving hot wall, the opposite effects must occur. These features are illustrated in Fig. 4 where the respective flow velocity profiles are shown for the wall velocities $v_w = 1$ m/s, $v_w = 0$ and $v_w = -1$ m/s in the case $\beta\Delta T = 0.22$. The corresponding solutions of Eq. (40) are $C/\tau_0 = 1.65052$, 1.724876 and 1.80501, respectively. The left and right cores move in this case with velocities $(V_L, V_R) = (1.579275, -0.579275)$, $(0.722768, -0.722768)$ and $(-0.103838, -0.896162)$, respectively. It is also worth emphasizing here that, while in the cases $v_w = 0$ and $v_w = 1$ m/s the velocity field is bidirectional, in the case $v_w = -1$ m/s it corresponds to a unidirectional downward flow.

5.3. Critical wall velocities

Concerning the effect of the applied shear on the core velocities V_L and V_R illustrated in Fig. 4, it is of physical interest to find the critical value of the wall velocity $v_w < 0$ for which the upward motion of the hot core gets stopped by the applied shear, i.e. V_L becomes zero. This value of v_w can be found as follows. One first substitutes $V_L = 0$ in the first Eq. (41) and one eliminates v_w between this equation and Eq. (40). Then, one solves the resulting equation

$$4S_+^3 - 2S_-^3 + 3S_-^2 - 1 = 0 \tag{49}$$

for C/τ_0. By substituting this value of $C/\tau_0 = (C/\tau_0)_{\text{crit}}$ in Eq. (40), one obtains the desired critical value $v_{w,\text{crit}}$ of v_w as

$$v_{w,\text{crit}} = -\frac{\upsilon\, Gr}{12H}.S_+^3\Big|_{C/\tau_0=(C/\tau_0)_{\text{crit}}} \tag{50}$$

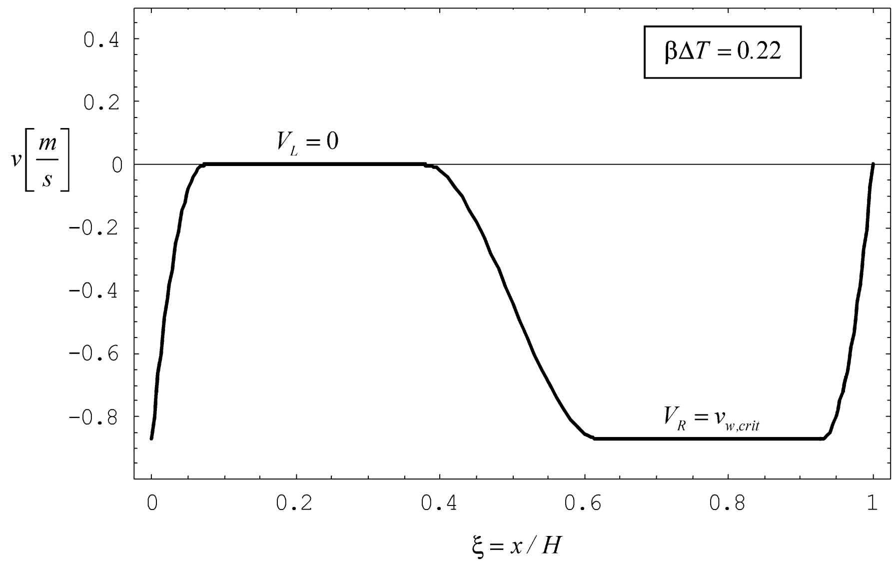

Fig. 5. Plot of the velocity profile (38) for $\beta\Delta T = 0.22$ and the critical value $v_{w,\mathrm{crit}} = -0.871866$ m/s of the wall velocity, where the hot core ceases to move.

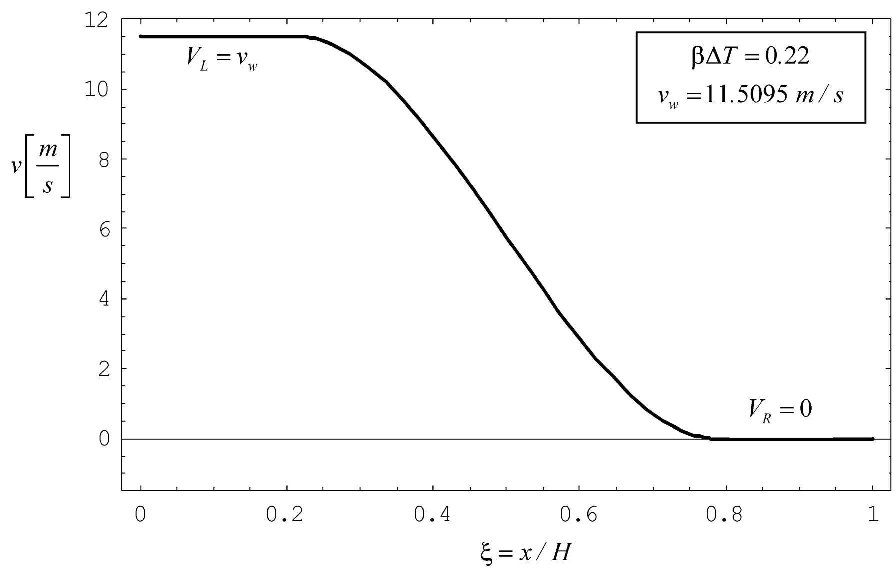

Fig. 6. Plot of the velocity profile of the three-domain flow field configuration corresponding to the wall velocity $v_w = 11.5095$ m/s for $\beta\Delta T = 0.22$. In this case the velocity of the right core is vanishing.

In this way, we arrive to the conclusion that the velocity field is bidirectional for $v_w > v_{w,\mathrm{crit}}$ and unidirectional for $v_w < v_{w,\mathrm{crit}}$. In the present case with $\beta\Delta T = 0.22$ one obtains $(C/\tau_0)_{\mathrm{crit}} = 1.794307$ and $v_{w,\mathrm{crit}} = -0.871866$ m/s. The velocity profile corresponding to $v_{w,\mathrm{crit}} = -0.871866$ is shown in Fig. 5.

With respect to the existence of a critical wall velocity with $v_w < 0$, there immediately occurs the question whether a critical wall velocity with $v_w > 0$ could exist, such that the downward motion of the right cold core gets stopped, i.e. V_R becomes zero. In contrast to the case $v_w < 0$, this phenomenon is not longer possible within a five-domain structure of the flow field, but only for the solution for $C/\tau_0 = 1$ of Eq. (40) which, as mentioned above, marks the crossover to a three-domain structure. Therefore, the corresponding values of the wall velocity are associated with the points of the dashed vertical line of Fig. 3. Thus, e.g. for $\beta\Delta T = 0.22$, the corresponding velocity of the upward moving hot wall is $v_w = 11.5095$ m/s. The velocity profile associated with this situation of the three-domain flow field is shown in Fig. 6.

5.4. The width of the cores

It is also of physical interest to examine the dependence of the width of the cores with solid body motion on the velocity v_w of the hot wall. First of all, it is seen that even for a non-symmetric velocity field, the (dimensionless) widths $\delta_L = \xi_2 - \xi_1$ and $\delta_R = \xi_4 - \xi_3$ of the left and right cores are always equal,

$$\delta_L = \delta_R \equiv \delta = \frac{S_- - S_+}{2} \tag{51}$$

This result is an immediate consequence of Eqs. (22) and (23). As an illustration, in Fig. 7 the change of δ has been plotted for

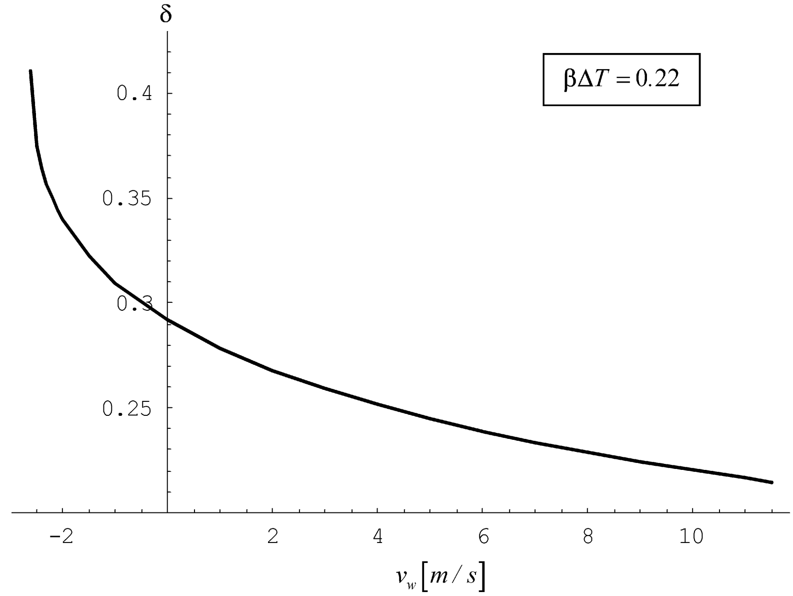

Fig. 7. Change of the dimensionless width of the cores for $\beta\Delta T = 0.22$, when, the wall velocity varies between -2.61806 and 11.5095 m/s (according to the third equation (48)).

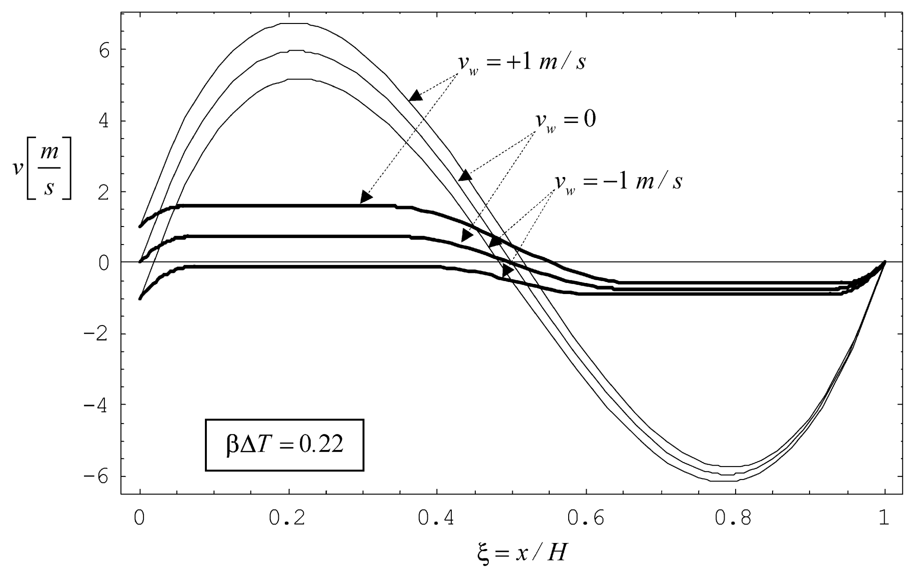

Fig. 8. Plot of the Bingham velocity profiles (38) (thick curves) and of the corresponding Newtonian ones (12) (thin curves) for $\beta\Delta T = 0.22$ and the wall velocities $v_w = 1$ m/s, $v_w = 0$ and $v_w = -1$ m/s, respectively.

$\beta\Delta T = 0.22$, when the wall velocity varies between -2.61806 and 11.5095 m/s (according to the third equation (48)). With increasing values of v_w, the width δ decreases from $\delta_{\max} = 0.410476$ at $v_w = -2.61806$ m/s to $\delta_{\min} = 0.214501$, reached at $v_w = 11.5094$ m/s.

5.5. Comparison with the Newtonian flow

In Fig. 8 the velocity profiles of the five-domain Bingham flows already shown in Fig. 4 (for $\beta\Delta T = 0.22$ and the wall velocities $v_w = 1$ m/s, $v_w = 0$ and $v_w = -1$ m/s) are compared to the velocity profiles of the corresponding Newtonian flows described by Eq. (12) (with the same values of υ and Gr, but $\tau_0 = 0$). While the Newtonian flows are always bidirectional, the five-domain Bingham flows show this feature only above the critical value of the wall velocity given by Eq. (50) (in the present example, $v_{w,\text{crit}} = -0.871866$ m/s). In the subcritical velocity range, $v_w < v_{w,\text{crit}}$, the Bingham flows are always unidirectional downward flows. According to Fig. 8, the maximum and minimum velocities of the two type of flows also differ substantially from each other.

Furthermore it is of interest to compare the kinetic energies per unit volume (17) for the two type of flows. The results of this comparison for the velocity profiles plotted in Fig. 8 are summarized in Table 1. As it is expected according to Fig. 8, in the case of the Bingham flows the values of

Table 1
Kinetic energies per unit volume KE/VOL [kJ/m^3] of the Newtonian and Bingham of respective velocity fields (12) and (38), for $\beta\Delta T = 0.22$ and three different wall velocities v_w

	$v_w = -1$ m/s	$v_w = 0$	$v_w = 1$ m/s
Newtonian flow	9.06	10.01	11.33
Bingham flow	0.207	0.227	0.648

KE/VOL [kJ/m^3] are substantially smaller than in the Newtonian case (in the present example one order of magnitude smaller.

6. Summary and conclusions

The effect of an externally applied shear stress on the free convection flow of a Bingham fluid in a parallel plane vertical channel has been investigated by analytical and numerical methods. The forcing shear stress was induced (in our mathematical model) by a uniform vertical motion of the hot wall in its own plane. The physically most interesting *five-domain configuration* of the velocity field of the emerging buoyant Couette–Bingham flow has been examined in detail. The main results of the paper can be summarized as follows.

1. The velocity field of the laminar Couette–Bingham flow has been given in a closed analytical form and its whole domain of existence has been found (see Eqs. (38), (41), (46) and Figs. 2 and 4).
2. For the *initiation temperature* of the five-domain Bingham flow predicted by Bayazitoglu et al., [1], a generally valid formula has been given (see Eq. (47) and Fig. 3).
3. The core velocities with rigid body motion of the Bingham material depend on the wall velocity sensitively (see Fig. 4). There exists a critical downward pointing wall velocity (given by Eq. (50)) for which the upward motion of the hot core is dropped. In this case the upward directed buoyancy force and the downward directed applied shear compensate each other exactly (see Fig. 5). The downward motion of the cold core, by contrast, can be stopped by an upward directed applied shear only within a *three-domain* flow regime (see Fig. 6). The hot and cold cores always possess the same width which, however, decreases with increasing wall velocity rapidly (see Fig. 7).
4. The velocity profile as well as the kinetic energy per unit volume of a Couette–Bingham flow differ from those of the corresponding Newtonian flows substantially (see Fig. 8 and Table 1).

We may conclude therefore, that the interplay between the buoyancy forces and the applied shear, can affect both the configuration of the flow field as well as the magnitude of the core velocities of the Bingham fluid sensitively. A future research opportunity is the investigation of the effect of an applied stress on the mixed convection Bingham flow considered for resting walls in an earlier paper of Patel and Ingham [3], as well as to the case of annular ducts [4,5].

Acknowledgements

One of the authors (E.M.) expresses his gratitude to the *Ministero Italiano dell'Università e della Ricerca* for supporting his collaboration in a *Progetto di Ricerca di Rilevante Interesse Nazionale* concerning the convection heat transfer in internal flows.

References

[1] Y. Bayazitoglu, P.R. Paslay, P. Cernocky, Laminar Bingham fluid flow between vertical parallel plates, Int. J. Thermal Sci. 46 (2007) 349–357.
[2] W.-J. Yang, H.-C. Yeh, Free convective flow of Bingham plastic between two vertical plates, Trans. ASME, J. Heat Transfer (May 1965) 319–320.
[3] N. Patel, D.B. Ingham, Analytic solutions for the mixed convection flow of non-Newtonian fluids in parallel plate ducts, Int. Comm. Heat Mass Transfer 21 (1994) 75–84.
[4] T.L. Guckes, Laminar flow of non-Newtonian fluid in an eccentric annulus, Trans. ASME J. Eng. Ind. 97 (1975) 498–506.
[5] N. Patel, D.B. Ingham, Mixed convection flow of a Bingham plastic in an eccentric annulus, Int. Comm. Heat Fluid Flow 15 (1994) 132–141.